Chalcogenide Letters Vol. 20, No. 2, February 2023, p. 165 - 175

Numerical simulation of the effect of gradual substitution of sulfur with selenium or tin with germanium in Cu_2ZnSnS_4 absorber layer on kesterite solar cell efficiency

N. Messei[a,*], M. S. Aida[b], A. Attaf[a], N. Hamani[a], S. Laznek[c]
[a]*Laboratory of Thin Films and Applications, Mohamed Khider University. Algeria*
[b]*Department of Physics, Faculty of Science, King Abdulaziz University, Saudi Arabia*
[4]*Department of SM, Faculty of Exact, Natural and Life Science, Mohamed Khider University. Algeria*

To enhance the efficiency of kesterite Cu_2ZnSnS_4 solar cell, different gradient strategies are investigated. Absorber layer gradient is obtained by partial substitution of sulfur with selenium or tin with germanium. The PV Parameters are calculated using the SCAPS1D program. The effect of the front, back, and double gradient on the cell parameters was investigated. We proposed also the fully graded gap absorber layer profile. The open-circuit voltage has increased to 1.040V, the fill factor has increased to 71.69%, and the efficiency has exceeded 22.95%. In contrast to other types of gradients, the short-circuit current density remains high (J_{sc}= 39.7mA / cm^2).

(Received November 24, 2022; Accepted February 17, 2023)

Keywords: Solar cell, Graded composition, Simulation, CZTS, Efficiency improvement, SCAPS1D

1. Introduction

Certainly, the major challenges in our contemporary life are those related to energy. The question always arises of how to get cheap and abundant energy from clean and renewable sources. One of the most important sources that send a huge amount of free and continuous energy to the earth is the sun. The way to convert this energy into electricity is through the use of well-known solar cells. Nowadays, mainstream thin-film photovoltaic technologies are copper indium gallium selenide (CIGS), cadmium telluride (CdTe), and amorphous silicon [1]. Solar cell with a CIGS absorber layer has shown good efficiency [1]. Unfortunately, mass production of this type of device faces the problem of gallium scarcity and indium toxicity. The kesterite copper zinc tin sulfide selenide $Cu_2ZnSn(S,Se)_4$ (CZTSSe) is one of the most promising materials used in solar cells as an absorber layer because it consists of safe and abundant elements in the earth's crust and has a large absorption coefficient (>$10^4 cm^{-1}$) [2-5]. Although CZTSSe is derived from CIGS and maintains its favorable photovoltaic properties, the power conversion efficiency (PCE) of the CZTSSe solar cell is limited to 12.6% [1, 6]. This record reached several years ago is still well below the Shockley-Queisser (SQ) limit of 31% efficiency under terrestrial conditions [7] and well below that of CIGS (22.6**%)** [6]. The champion device with a 1.13 eV band gap only achieved an open circuit voltage (V_{oc}) of 0.513 V and a short circuit current (J_{sc}) of 35.2 mA cm^{-2} [5]. It is well-known that the PCE of $Cu_2ZnSn(S, Se)_4$ solar cells is mainly limited by the lower V_{oc}, which has become a major challenge in this field [8, 9]. The Investigation into the origin of this deficit is required to achieve further progress in the device efficiency, therefore establishing $Cu_2ZnSn(S, Se)_4$ as a low-cost, earth-abundant alternative to CIGS and CdTe solar cells.

There are two types of causes that negatively affect the efficiency of the solar cell. The first type is related to the properties of the absorber layer material. We can mention Cationic disorder, the formation of complex secondary phases, and the presence of intrinsic defects [10]. The second type is related to the design of the solar cell itself and its ability to separate charge carriers and direct electrons to the external circuit. We can mention the undesirable band offset at back-contact/CZTS, and the problem of non-ideal band alignment at the CZTS/CdS interface [11-

* Corresponding author: messei_nadia@yahoo.fr
https://doi.org/10.15251/CL.2023.202.165

13]. The CZTS/CdS interface should be studied carefully to achieve high-performance solar cells. Three cases are possible at this interface i) spike-like or positive conduction band offset CBO when The conduction band minimum $CBM_{(n)}$ of the n-type semiconductor is higher than $CBM_{(p)}$ the conduction band minimum of the p-type semiconductor, ii) cliff-like or negative CBO when the position of the $CBM_{(n)}$ is lower than the $CBM_{(p)}$, iii) flat-band. The $CBM_{(n)}$ must be slightly higher than the $CBM_{(p)}$ at the interface or at least flat-band because the spike-like barrier acts as a notch against photo-generated carriers in the absorber layer preventing recombination losses [14]. The flexibility of anion and cation substitution in CZTSSe solar cells could offer a variety of options for band alignment at the interface absorber/CdS and the creation of BSF for the reason that the CBM of CZTSSe semiconductor changes by changing its composition [15]. This work aims to exploit this feature to improve the efficiency of the CZTSSe solar cell using numerical simulation. One way to facilitate the study of CZTSSe solar cell is to extend the results of CIGS solar cell to CZTSSe solar cell simply by replacing CIGS layer with CZTSSe layer. It was reported that adjusting the conduction band offset of window/CIGS layers can lead to a high performance of CIGS solar cell [14, 16]. Besides, CIGS absorber layer-graded composition is a key for high-performance solar cells [17-22].

It was reported that the gradual substitution of sulfur (S) atoms by selenium atoms (Se) enables a gradual change of both CBM and VBM simultaneously [23] and the gradual substitution for Sn atoms by Ge atoms changes just the CBM [24]. The S/Se composition grading is not a good option for back band grading, however, it is appropriate and effective for front band grading, because the descending VBM near the back contact acts as a barrier for holes collection and this negatively affects the performance of the solar cell [15]. On the other hand, a beneficial back band grading can be achieved by Ge/Sn grading which only changes the conduction band. A gradual CBM strategy can be applied to the CZTSSe absorber layer to adjust the band alignment at the interface CZTSSe/CdS.

2. Modeling and simulation

2.1. Simulation program

In this work, the device simulations are carried out using the simulation package, SCAPS1D, a one-dimensional solar cell simulator. A variety of interpolation laws are available to set the position-dependent composition y of each layer: y(x) [25]. These interpolation laws can also be applied to set the band-gap $E_g(y)$ and the electron affinity $\chi(y)$ and all-important semiconductor properties [25]. So, the combination with the composition profile y(x) gives the 'grading' of these parameters, e.g. $E_g(x) = E_g[y(x)]$ [25]. Several parameters could be calculated. In this study, we focused on the solar cell's electric parameters (V_{oc}, J_{sc}, FF, and η) (under 1.5 AM conditions).

2.2. Device structure

The structure under study (p-CZTSSe/n-CdS/i-ZnO/ZnO: Al) with the optimized thickness of each layer and energy band diagram of our solar cell is shown in fig. 1. Layers properties are illustrated in table. 1. Contacts are assumed ohmic. At the contacts, a (wavelength-dependent) reflection/transmission can be set. The reflection at the back surface has a tiny influence on the achievable J_{sc} and becomes noticeable only if the absorber is fairly thin.

The density of intrinsic defects in the absorber layer must be optimized to define guidelines for improving cell performance. The potential defects in kesterite structure that are formed during the growth of CZTSSe crystals include vacancies (V_{Cu}, V_{Zn}, V_{Sn}, and $V_{S(e)}$), interstitials (Cu_i, Zn_i, Sn_i, and $S(e)_i$), and the antisites (Cu_{Zn}, Zn_{Cu}, Cu_{Sn}, Sn_{Cu}, Zn_{Sn}, and Sn_{Zn})[10,15]. In addition, the donor and acceptor defects may also attract each other, forming defect clusters because of their lower formation energy compared to antisite defects formation energy [10,15, 26]. All of the above-mentioned defects can exist in the CZTSSe layer, but with different concentrations, depending on the deposition process. They directly influence the generation, separation, and recombination of electron-hole pairs. On the other hand, intrinsic defects are also responsible for the self-doping of a semiconductor influencing the carrier

concentration and can influence the electrical conductivity, the serial resistance, and thus both FF and Voc [10, 15, 26]. In order to model non-radiative recombination (S-R-H) in $CZTS_{1-y}Se_y$ layer, a Gaussian distribution of defects was established in the gap and centered in its midpoint as shown in table. 2. There is an inverse proportion between defect density and cell efficiency. As shown in fig. 2 the efficiency starts to decrease when the density exceeds 10^{14} cm^{-3}. Optimization of the defect density is a key to efficiency improvement.

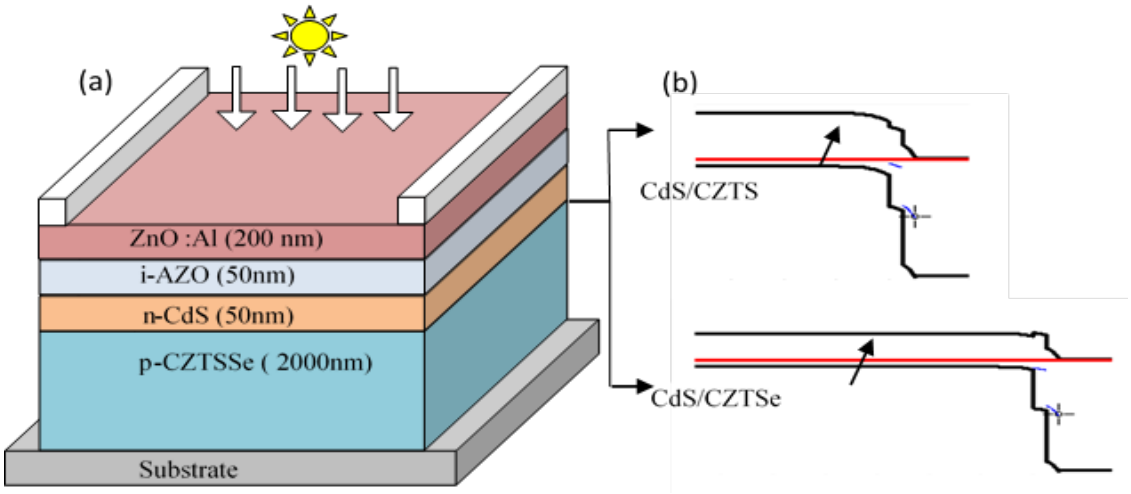

Fig. 1. The CZTSSe thin film solar cell: (a) structure of the cell (b) Band alignment at the CdS/CZTSSe and CdS/CZTS interfaces from SCAPS1D.

Table 1. Properties of the CZTSSe solar cell used in simulation at 300° k [32-36]

layer	p-CZTS	p-CZTSe	n-CdS	i-ZnO	n+-ZnO
Thickness (µm)	2.00	2.00	0.05	0.05	0.20
The optical band gap (eV)	1.5	0.99	2.42	3.37	3.37
Electric permittivity	6.5	8.6	10	9	9
Electron affinity (eV)	4.1	4.35	4.2	4.5	4.5
Electron thermal velocities (m/s)	100	100	100	100	100
hole thermal velocities (m/ s)	$1x10^7$	$1x10^7$	$1x10^7$	$1x10^7$	$1x10^7$
electron thermal velocities (m/ s)	$1x10^7$	$1x10^7$	$1x10^7$	$1x10^7$	$1x10^7$
CB effective density of states (cm^{-3})	8.1×10^{16}	7.9×10^{17}	$2.0x10^{19}$	$9x10^{18}$	$2.2x10^{18}$
VB effective density of states (cm^{-3})	1.5×10^{19}	4.5×10^{18}	$1.5x10^{18}$	$4x10^{18}$	$1.8x10^{19}$
Shallow uniform donor density N_A (cm^{-3})	2.10^{16}	2.10^{16}	/	/	/
Shallow uniform acceptor density N_D (cm^{-3})	/	/	1.10^{16}	1.10^{17}	1.10^{19}

Table 2. Defects parameters used in our work: (a) indicates acceptor and (d) donor.

type	(a)	(a)	(d)	(d)	(d)
Energy level above E_V (eV)	0.75	0.50	1.20	1.65	1.65
Density (cm^{-3})	10^{14}	10^{14}	10^{16}	10^{17}	10^{18}

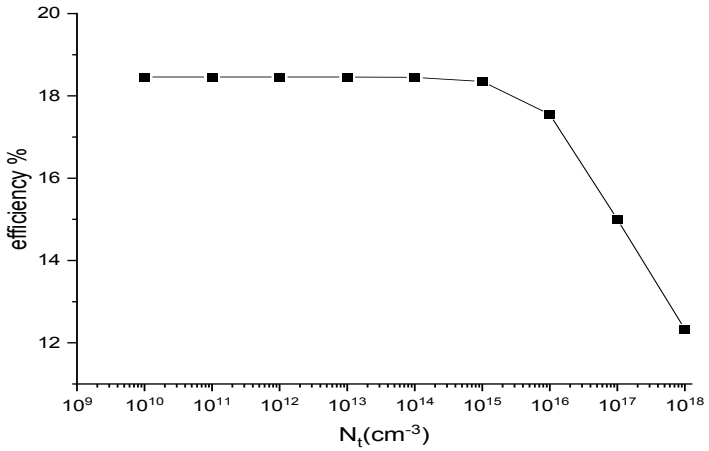

Fig. 2. The change of efficiency of uniform CZTS solar cell with the density of defects in the absorber layer.

2.3. Optical energy gap and electron affinity after atoms substitution

Values of optical energy gap (Eg) and electron affinity (χ) used to build the graded solar cell investigated in this work are collected from different theoretical and experimental references. In the component $Cu_2ZnSn(Se_yS_{1-y})_4$, y is the molar fraction Se/(Se+S). The gradual substitution of S by Se in kesterite $CZTS_{1-y}Se_y$ decreases the band gap linearly and obeys Vegard's rule. This is confirmed by Calculated [27-30] and experimental results summarized in Ref [31]. In this work, the Eg of Kesterite $CZTS_{1-y}Se_y$ was described by (eq. (1)) mentioned in ref [30].

$$Eg = 1.505(1-y) +0.984y-0.123y(1-y) \quad (1)$$

When the composition changes linearly from CZTS to CZTSe, "y" gradually changes from 0 to 1, and the band gap energy changes from 1.49 to 0.98 eV. According to refs [32-34], the conduction band offset (CBO) is "spike-like" for CZTSe/CdS interface and "cliff-like" for CZTS/CdS. In fact, all kesterite $CZTS_{1-y}Se_y$ properties are affected by the change in the S/Se ratio. In the same way, the gradual substitution of the Tin (Sn) atom by the Germanium (Ge) atom in kesterite CZTS increases the band-gap energy linearly. In the component $Cu_2ZnGe_zSn_{1-z}Se_4$(CZTGSe), (z) means the molar fraction Ge/(Ge+Sn). the Eg is mainly the same in Many studies [22, 37-39]. In this work, we used Eg values of Ref [39]. The Eg of CZGTSe linearly increased with increasing Ge content from 0.98 eV for CZTSe (z = 0) to 1.37 eV for CZGSe (z = 1) with increasing Ge content. In the next discussion, we will use this notation: CBM (VBM) for the conduction (valence) band minimum (maximum) energy levels relative to the vacuum level, respectively. CBO and VBO are expressed by the following equations:

$$CBO = CBM_{(CZTGSSe)} - CBM_{(CdS)} \quad (2)$$

$$VBO = VBM_{(CdS)} - VBM_{(CZTGSSe)} \quad (3)$$

In SCAPS program the value of CBM is expressed by the electron affinity χ consequently, the value of VBM is the sum of the electron affinity and the optical energy gap:

$$CBO = \chi_{(CZTGSSe)} - \chi_{(CdS} \quad (4)$$
$$VBO = (\chi_{(CdS)}+Eg_{(CdS)})-(\chi_{(CZTGSSe)}+Eg_{(CZTGSSe)})$$

After rearrangement:

$$VBO= -CBO + (Eg_{(CdS)} - Eg_{(CZTGSSe)}) \quad (5)$$

Following ref [36] and as shown in fig.3, the $VBM_{(CZTS1-ySey)}$ is almost linearly down-shifting along with Se composition, and the variation range is small (~0.15eV) while $CBM_{(CZTS1-ySey)}$ is also almost linearly down-shifting along with Se composition, but the variation range is more important (~0.35 eV). The VBM does not change by substitution of Ge for Sn in $Cu_2ZnSnSe_4$. Fig.3 shows the VBM $_{(CZTGSe)}$ level from the vacuum level. CBM $_{(CdS)}$ is shown for reference. $CBM_{(CZTGSe)}$ level linearly increases from −4.22 eV for $Cu_2ZnSnSe_4$ (z = 0) to −3.88 eV for $Cu_2ZnGeSe_4$ (z = 1) [39]. The value of CBM is included from the fact that VBM is not sensible to (Ge) ratio so:

$$\chi_{(CZGSe)} + Eg_{(CZGSe)} = \chi_{(CZTSe)} + Eg_{(CZTSe)} \quad (6)$$

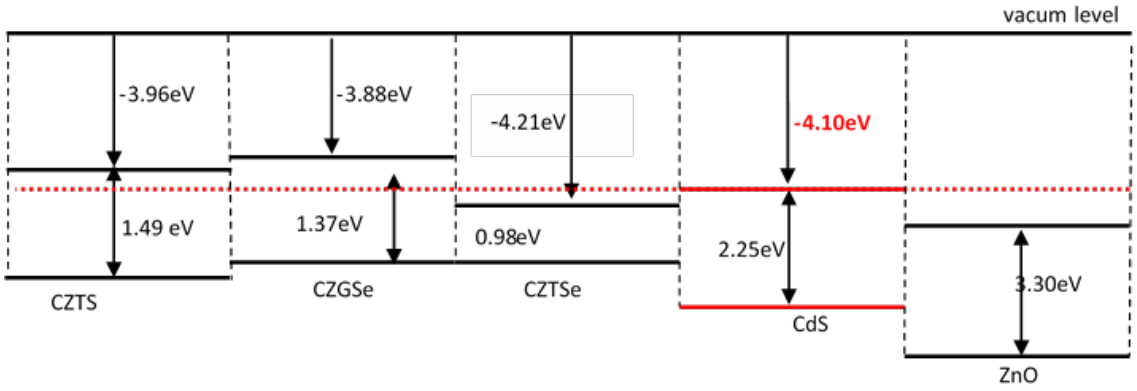

Fig.3. Energy levels of VBM and CBM from the vacuum level of CZTS, CZTSSe, CZGSe, CdS, and ZnO layers.

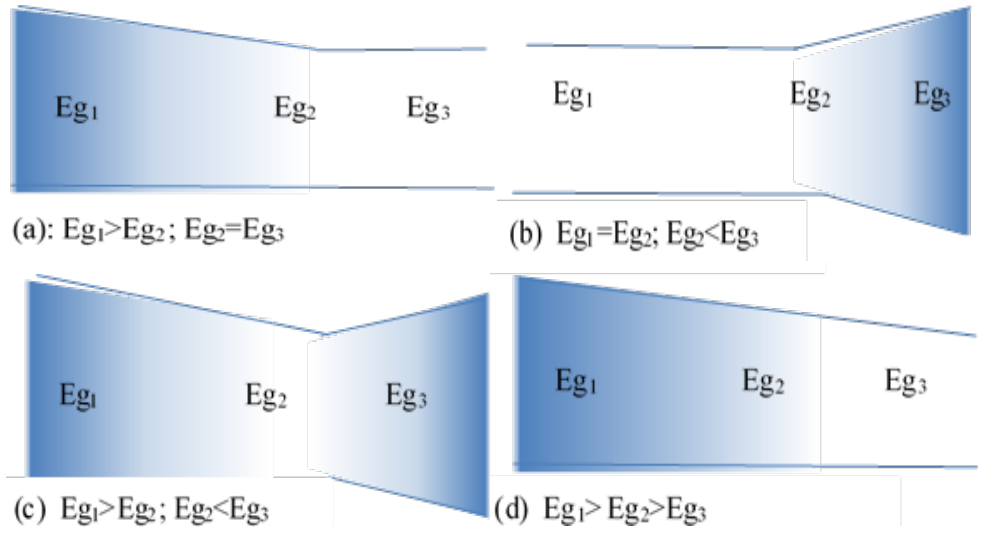

Fig. 4. Absorber layer gradual gap profiles (a) back gradual gap (b) front gradual gap (c) notch-like gradual gap (d) fully gradual gap (proposed in this work).

3. Result and discussion

3.1. Uniform CZTSe, CZTG, and CZTS cells

To determine the effect of the gradient on the solar cell's performance, one must compare the parameters of the graded cell with those of a uniform cell. Possible uniform cells are cells with uniform CZTSe (y=1, z=0), uniform CZTG(z=1), and uniform CZTS(y=0). The Open circuit voltage (V_{oc}) in V, the density of short circuit current (J_{sc}) in mA/cm^2, the fill factor (FF %), and

the efficiency (η %) of uniform solar cells were carried out (under 1.5 AM conditions) and illustrated in the table. 3. The ratio of Se and Ge in the absorber material affects both the J_{sc} and the V_{oc} of the cell with a uniform absorber layer. Higher Eg leads to higher V_{oc} and lower J_{sc}, this is very clear in the three cells. The grading of absorber layer parameters is not the only source of the trade-off between J_{sc} and V_{oc}. Another parameter to be taken into consideration here is the CBO at the contact $CZTS_{1-y}Se_y$/CdS as shown in fig.3.

As shown in table. 3, the CZTS cell has the highest efficiency of 18.24 %, the lowest J_{sc} of 28.18 mA/cm^2, and the highest V_{oc} of 1.040 V. The CZTSe cell has the lowest efficiency of 14.64%, the highest J_{sc} of 48,56 mA/cm^2, and the lowest V_{oc} of 0,620V. In this work, we have investigated the traditional gradient profiles: the back, the front, and the double gradient (notch-like). Besides, we have proposed an absorber layer with a fully gradual gap (Fig. 4). In all that we will discuss later, we consider the uniform CZTSe solar cell as the basic cell with an efficiency of 14.64 % as shown in table. 3. We use the term “beneficial” if the efficiency of the cell is more than the efficiency of the uniform CZTS solar cell (18.24%), and it is "not beneficial" if the efficiency of the cell is less than that. We will use the term the “back” of the absorber is the region before the substrate and the “front” is the region before the contact with CdS.

Table 3. Parameters of uniform cells.

Absorber	V_{oc}(V)	J_{sc}(mA/cm2)	FF %	Efficiency %
CZTS	1,040	28,18	62,52	18,45
CZGeSe	0,926	31,62	56,52	16,56
CZTSe (basic cell)	0,620	48,56	48,43	14,64

3.2. Back gradient: substitution of Sn with Ge

In this section, we consider the back gradient in which the composition of CZTGSe changes linearly from the back to the front by changing the Ge/(Ge+Sn) ratio.

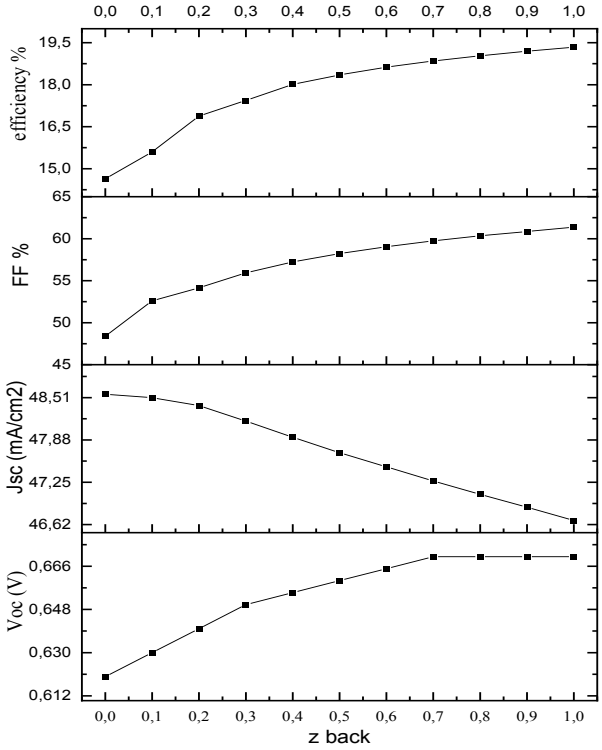

Fig. 5. Influence of the back gradient on the V_{oc}, J_{sc}, FF, and η of CZTGSe solar cell (z is graded from 0 to 1).

To achieve this, we fix the value of the band gap at the front at the lowest possible value of 0.98 eV which corresponds to z = 0 (CZTSe) and we change the value of z from 0 to 1(CZGSe) at the back. Fig. 5 shows an improvement in V_{oc} to 0.641eV, a slight decrease in J_{sc} to 46.68mA/cm^2, and a clear increase in efficiency to 19.34%. This amelioration can be explained by the quasi-electric field (created by the back gradient) which facilitates the collection of minority carriers generated far away from the junction region. So, we consider that the back gradient is beneficial.

This result can be improved by optimizing the depth to which the gradient is applied. As shown in Fig. 6, the depth of 1.5µm gives the best efficiency up to 19.70 %. Based on this result, we have divided the absorber layer (2 µm) into two parts, one with a length of 1.5 µm (part 1), and the second with a length of 0.5 µm (part 2). This division will be used in the next section.

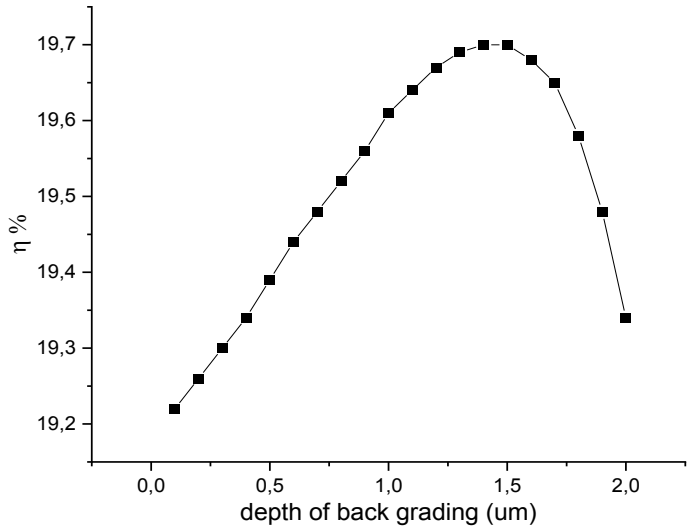

Fig. 6. Influence of the depth of "back gradient" on the efficiency of CZTSSe solar cell (x is increased from 0 to 2 µm).

3.3. Front gradient: substitution of S by Se

In contrast to the back gradient, in the front gradient, the composition of CZTSSe changes linearly from the front to the back by changing the Se/(Se+S) ratio. To achieve this latter, we fix the value of the band gap at the back at the lowest possible value of 0.98 eV, which corresponds to y=1(CZTSe), and we change the value of y from 1 to 0(CZTS) at the front. Fig. 7 shows a decrease in J_{sc} from 48.56 to 24.52 mA/cm^2 and V_{oc} increases from 0.623 to 1.008 V. The best value of FF is achieved at y=0.6. The efficiency of the cell decreases dramatically from 14.24 to 11.17%. The amelioration of V_{oc} is explained by the increase in the recombination energy barrier at the junction interface. Besides, the front gradient creates an electric field in an opposite direction to the electric field created by the junction of the cell (CdS/CZTSSe) resulting in a decrease in J_{sc}. The font grading is not beneficial for the CZTSSe solar cell.

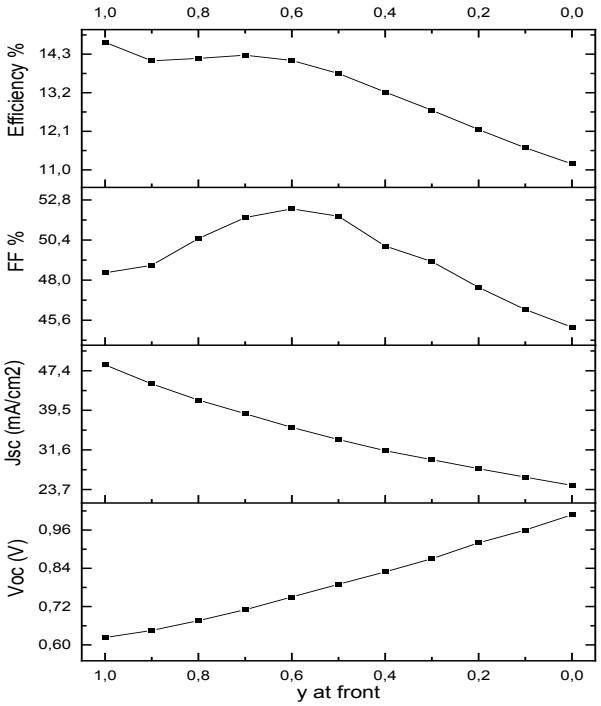

Fig. 7. Influence of the front gradient V_{oc}, J_{sc}, FF, and η of CZTGSe solar cell (y is graded from 1 to 0

3.4. Notch-like gradient

To create a double gradient (notch-like) profile we apply a front gradient only in the second part of the absorber layer as shown in Fig. 4(c). The notch-like gradient breaks the cell efficiency as it drops to 7.81%. This occurs because of the barrier created just before the CdS/CZTSSe interface, which makes it difficult for carriers to reach the junction. This cancels out the improvement caused by the back gradient. As shown in Fig.8, the double gradient is also not beneficial to cell performance

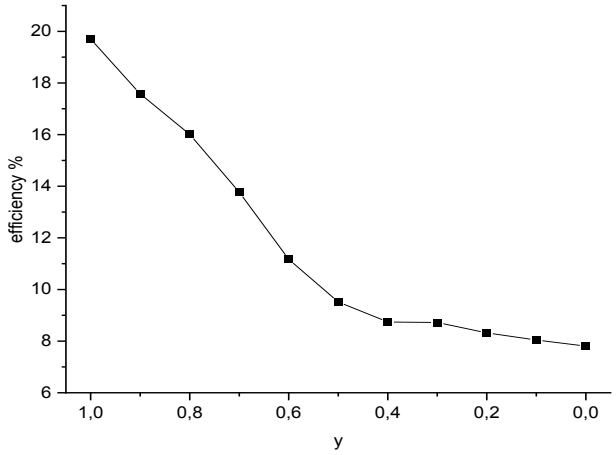

Fig. 8. Influence of the double gradient on the efficiency of CZTSSe solar cell (y is graded from 1 to 0).

3.5. CZTSSe or CZTGSe Absorber layer with a full gradient

As mentioned in the introduction, it was assumed that the front gradient and the double gradient would benefit the CZTSSe cell. When the front gradient is implemented, we overcome the problem of conduction band alignment at the interface CdS/CSTSSe but the result of the simulation was disappointing due to the drop in Eg_2 as shown in Fig. 4.

To overcome the deficit in the double-graded structure, we resort to raising Eg_2 while maintaining the front gradient. By applying this strategy, we get the fully graded profile shown in fig. 4(d) characterized by $Eg_3 < Eg_2 < Eg_1$. In this section, atom substitution is the same to create the front gradient and the back gradient. The fully graded model can be obtained in two cases CZTSSe and CZTGSe absorber. Significant improvement in the efficiency of CZTSSe cell up to 22.95 % at y=0.4 and up to 21.82 % at z=0.5 in the efficiency of CZTGSe cell. At the first hand, The V_{oc} increases almost linearly with increasing Eg_3. The V_{oc} almost doubles (V_{oc}=1.041V) when y=0 at the front and y=1 at the back of the CZTSSe absorber layer as shown in Fig. 9. On the other hand, The J_{sc} decreases almost linearly with increasing Eg_3 (J_{sc}=28.18 mA/cm^2). A similar improvement occurs in the CZTGSe cell where V_{oc} increases to 0.920V and J_{sc} decreases to 31.62 mA/cm^2. When y=0.4 we notice a significant improvement in the efficiency of CZTSSe cell up to 22.95 % and in FF of 71.69%. Also, in the CZTGSe cell when z = 0.5, there is a significant improvement in the efficiency of up to 21.82 % and in FF of 70.36%. As a result of the aforementioned values, we say that the fully graded model proposed in this work gave the highest cell efficiency and the highest V_{oc}.

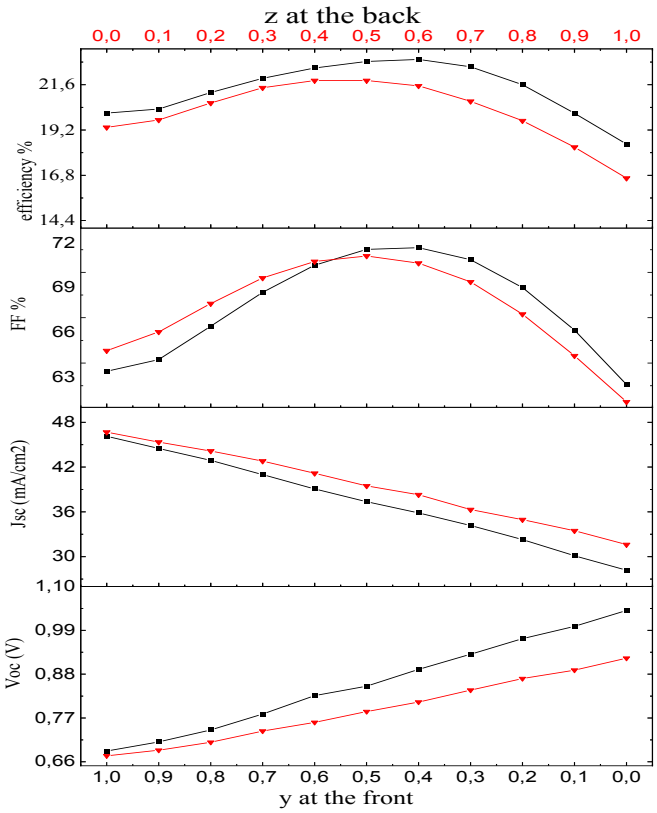

Fig. 9. Influence of the full gradient profile (proposal profile) on the V_{oc}, J_{sc}, FF, and η of the solar cell (■) is for CZTSSe and (▼) for CZTGSe absorber layer.

4. Conclusion

This analytical study aims to improve the efficiency of Kesterite CZTSSe solar cells by applying different gradient strategies for the absorbing layer. The simulation was carried out using the SCAPS1D program. The front gradient, the back gradient, and the double gradient were investigated. The J_{sc}, the V_{oc}, the FF, and the efficiency of graded solar cells were compared with those of uniform cells. The simulation results showed that the back gradient is beneficial for cell performance in contrast to the front gradient and the double gradient. Double gradient glitches are avoided and we get a new gradient model. Finally, it may be concluded that by adopting a fully

graded absorber layer the performance of the CZTSSe solar cell can be improved. A cell with 22.95% efficiency, JSC=39.7mA/cm^2, V_{oc}= 1.040V, and FF =71.69% can be achieved.

Acknowledgments

The authors would like to acknowledge gratefully M. Burgelman from ELIS, the University of Gent for giving us permission to use SCAPS1D.

References

[1] M. Green, E. Dunlop, J. Hohl-Ebinger, M. Yoshita, N. Kopidakis, X. Hao, Progress In Photovoltaics: Research And Applications. 29 (2021) 657-667; https://doi.org/10.1002/pip.3444

[2] K. Ito. Copper Zinc Tin Sulfide-Based Thin Film Solar Cells. Wiley, (2014); https://doi.org/10.1002/9781118437865

[3] X. Liu, Y. Feng, H. Cui, F. Liu, X. Hao, G. Conibeer et al., Progress In Photovoltaics: Research And Applications. 24 (2016) 879-898; https://doi.org/10.1002/pip.2741

[4] D. Mitzi, O. Gunawan, T. Todorov, D. Barkhouse, Philosophical Transactions of The Royal Society A: Mathematical, Physical And Engineering Sciences. 371 (2013) 20110432; https://doi.org/10.1098/rsta.2011.0432

[5] S. Kodigala. Thin film solar cells from earth abundant materials. Amsterdam: Elsevier, (2014); https://doi.org/10.5772/51734

[6] W. Wang, M. Winkler, O. Gunawan, T. Gokmen, T. Todorov, Y. Zhu et al. Advanced Energy Materials. 4 (2013) 1301465; https://doi.org/10.1002/aenm.201301465

[7] W. Shockley, H. Queisser, Journal of Applied Physics. 32 (1961) 510-519; https://doi.org/10.1063/1.1736034

[8] J. Moore, C. Hages, R. Agrawal, M. Lundstrom, J. Gray, Applied Physics Letters. 109 (2016) 021102; https://doi.org/10.1063/1.4955402

[9] T. Gokmen, O. Gunawan, T. Todorov, D. Mitzi, Applied Physics Letters. 103 (2013) 103506; https://doi.org/10.1063/1.4820250

[10] M. Minbashi, A. Ghobadi, E. Yazdani, A. Ahmadkhan Kordbacheh, A. Hajjiah, Scientific Reports. 10 (2020); https://doi.org/10.1038/s41598-020-75686-2

[11] J. Scragg, T. Kubart, J. Wätjen, T. Ericson, M. Linnarsson, C. Platzer-Björkman, Chemistry Of Materials. 25 (2013) 3162-3171; https://doi.org/10.1021/cm4015223

[12] A. Crovetto, O. Hansen, Solar Energy Materials And Solar Cells. 169 (2017) 177-194; https://doi.org/10.1016/j.solmat.2017.05.008

[13] C. Yan, J. Huang, K. Sun, S. Johnston, Y. Zhang, H. Sun et al., Nature Energy. 3 (2018) 764-772; https://doi.org/10.1038/s41560-018-0206-0

[14] T. Minemoto, T. Matsui, H. Takakura, Y. Hamakawa, T. Negami, Y. Hashimoto et al., Solar Energy Materials And Solar Cells. 67 (2001) 83-88; https://doi.org/10.1016/S0927-0248(00)00266-X

[15] M. He, C. Yan, J. Li, M. Suryawanshi, J. Kim, M. Green et al., Advanced Science. 8 (2021) 2004313; https://doi.org/10.1002/advs.202004313

[16] C. Yan, F. Liu, N. Song, B. Ng, J. Stride, A. Tadich et al., Applied Physics Letters. 104 (2014) 173901; https://doi.org/10.1063/1.4873715

[17] Y. Nagoya, K. Kushiya, M. Tachiyuki, O. Yamase, Solar Energy Materials And Solar Cells. 67 (2001) 247-253; https://doi.org/10.1016/S0927-0248(00)00288-9

[18] Y. Hirai, Y. Hidaka, Y. Kurokawa, A. Yamada, Japanese Journal of Applied Physics. 51 (2012) 10NC03; https://doi.org/10.1143/JJAP.51.10NC03

[19] T.-Y. Lin, C.-H. Lai, in 2015 IEEE 42nd Photovolt. Spec. Conf., IEEE, New Orleans, LA 2015, pp. 1-4.

[20] M. Gloeckler, J. Sites, Journal of Physics and Chemistry of Solids. 66 (2005) 1891-1894; https://doi.org/10.1016/j.jpcs.2005.09.087
[21] A. Morales-Acevedo, Energy Procedia. 2 (2010) 169-176; https://doi.org/10.1016/j.egypro.2010.07.024
[22] O. Lundberg, M. Edoff, L. Stolt, Thin Solid Films. 480-481 (2005) 520-525; https://doi.org/10.1016/j.tsf.2004.11.080
[23] S. Chen, X. Gong, A. Walsh, S. Wei, Applied Physics Letters. 94 (2009) 041903; https://doi.org/10.1063/1.3074499
[24] T. Nagai, S. Kim, H. Tampo, K. Tanigawa, Y. Iwamoto, H. Hamada et al., Physica Status Solidi (RRL) - Rapid Research Letters. 14 (2020) 1900708; https://doi.org/10.1002/pssr.201900708
[25] M. Burgelman, J. Marlein, Proceedings of the 23rd European Photovoltaic Conference, Valencia, Spain . (2008) 2151-2155.
[26] S. Chen, A. Walsh, X. Gong, S. Wei, Advanced Materials. 25 (2013) 1522-1539; https://doi.org/10.1002/adma.201203146
[27] S. Chen, X. Gong, A. Walsh, S. Wei, Applied Physics Letters. 94 (2009) 041903; https://doi.org/10.1063/1.3074499
[28] J. Paier, R. Asahi, A. Nagoya, G. Kresse, Physical Review B. 79 (2009); https://doi.org/10.1103/PhysRevB.79.115126
[29] S. Chen, X. Gong, A. Walsh, S. Wei, Physical Review B. 79 (2009); https://doi.org/10.1103/PhysRevB.79.165211
[30] Z. Zhao, Q. Liu, X. Zhao, Journal of Alloys and Compounds. 618 (2015) 248-253; https://doi.org/10.1016/j.jallcom.2014.08.213
[31] S. Das, K. Mandal, Materials Research Bulletin. 57 (2014) 135-139; https://doi.org/10.1016/j.materresbull.2014.04.073
[32] J. He, L. Sun, S. Chen, Y. Chen, P. Yang, J. Chu, Journal of Alloys and Compounds. 511 (2012) 129-132; https://doi.org/10.1016/j.jallcom.2011.08.099
[33] S. Chen, A. Walsh, J. Yang, X. Gong, L. Sun, P. Yang et al., Physical Review B. 83 (2011); https://doi.org/10.1103/PhysRevB.83.125201
[34] A. Nagoya, R. Asahi, G. Kresse, Journal of Physics: Condensed Matter. 23 (2011) 404203; https://doi.org/10.1088/0953-8984/23/40/404203
[35] C. Persson, Journal of Applied Physics. 107 (2010) 053710; https://doi.org/10.1063/1.3318468
[36] I. Repins, N. Vora, C. Beall, et al, Materials Research Society Spring Meeting San Francisco, California (2011), NREL/CP-5200-51286.
[37] S. Chen, A. Walsh, Y. Luo, J. Yang, X. Gong, S. Wei, Physical Review B. 82 (2010); https://doi.org/10.1103/PhysRevB.82.195203
[38] S. Kumar, D. Sharma, B. Joshi, S. Auluck, AIP Advances. 6 (2016) 125303; https://doi.org/10.1063/1.4971323
[39] K. Tsuji, T. Maeda, T. Wada, Japanese Journal of Applied Physics. 57 (2018) 08RC21; https://doi.org/10.7567/JJAP.57.08RC21